Modeling and Simulation of Partial Oxidation of Methanol to Formaldehyde on FeO/MoO₃ Catalyst in a Catalytic Fixed Bed Reactor

Olatunde, Abayomi Olaniyi*⁺***; Olafadehan, Olaosebikan Abidoye;***
Usman, Mohammed Awwal
Department of Chemical and Petroleum Engineering, University of Lagos, Lagos, NIGERIA

ABSTRACT: *A two-dimensional mathematical model was developed for a porous heterogeneous catalytic fixed bed reactor. The model took into account the effect of heat generated by adsorption of reactants on the catalyst surface and heat transfer from the fluid phase to the surroundings which have a significant effect on reactor performance, especially at reactor hotspot. The developed model predicted the partial oxidation of methanol to formaldehyde on FeO/MoO₃ catalyst, a complex reaction system. Excellent agreement was achieved when the resultant simulated results were compared with experimental data in the literature. The proposed model predicted the location of the hotspot at a dimensionless distance of 0.4413 (= 0.0309 m) the same as the experiment value but with a temperature of 619 K compared with an experimental value of 622 K. The conventional heterogeneous and pseudo-homogeneous models predicted the hotspot temperature to be about 8 K and 34 K lower than the experimental value respectively.*

KEYWORDS: *Heterogeneous; Pseudo-homogeneous; Non-isothermal; Orthogonal collocation; Hotspot.*

INTRODUCTION

Most of the reactions taking place in a catalytic fixed bed reactor are complex. These can be in the form of highly exothermic reactions or highly endothermic reactions. Usually, when a highly exothermic reaction takes place in a catalytic fixed bed reactor, some problems related to the operation of the reactor always occur since most of the chemical reaction terms are a highly non-linear function of temperature and concentration and the value of heat may vary in the large amount. When heat is produced faster than the rate it leaves the reactor walls, a rapid increase in the reactor temperature results [1]. This excessive heat in the reactor is referred to as 'temperature runaway', which causes some deleterious effects in the reactor. These include the promotion of undesired side reactions, catalyst deactivation by sintering and productivity loss, and reduction of product selectivity. Thus, there is a need to develop a model that predicts the outer-tube wall temperature profile for a given set of inputs, and the effect of heat loss through the wall on the magnitude of hotspot temperature which will help plant operators to reduce the risk of the reactor failure. Also, there is continuous generation or consumption of heat due to enthalpies of adsorption and chemical reaction. The heat transfer that takes place during the adsorption of reactants

on the catalysts, the surface contributes to the thermal behavior of the fixed bed reactor as it increases the temperature of the reactor [2-3]. It is important to develop a model that incorporates the effect of heat generated by adsorption of reactants on the catalyst surface in the reactor with a view to integrating its effect on the hotspot and runaway phenomena.

Several models have been proposed in the literature to study the behavior of fixed bed reactors. The models are grouped into two major categories namely: the pseudo-homogeneous and heterogeneous models. Many works have been done on the modeling and simulation of catalytic packed bed tubular reactors using a two-dimensional pseudo-homogeneous model [4-14]. They assumed the catalyst surface to be totally exposed to the bulk fluid conditions, that is, there is no fluid-to-particle heat and mass transfer resistance between the solid and the fluid phases. This implies there is a negligible difference between the fluid and solid phase conditions and mild radial concentration and temperature profiles. However, there are some cases when the differences between conditions in these phases are significant mostly highly exothermic reactions which are common in industries, hence heterogeneous models have to be considered. The conventional heterogeneous model developed by [11,15-18] although caters to the defects in the pseudo-homogeneous models but still failed to explain explicitly the effects of heat loss from the fluid phase *via* the wall to the surrounding and the effect of heat generated by adsorption of reactants on the catalyst surfaces both of which have effects on the location and magnitude of hotspots and temperature runaway phenomena.

This work will develop a two-dimensional heterogeneous reactor model that will that incorporate the effect of heat generated by adsorption of reactants on the catalyst surface in the reactor and also explicitly predicts the effect of outer-tube wall temperature profile for a given set of inputs, and the effect of heat loss through the wall. This will be compared with two-dimensional pseudo homogeneous and conventional heterogeneous models. The developed models will be used to predict the reaction process for partial oxidation of methanol to formaldehyde on FeO/MoO_3 catalyst.

Two-dimensional pseudo-homogeneous model

This model considers concentration and temperature profiles in the bulk fluid phase both in the axial and radial directions. It considers in addition to convection flow, heat, and mass dispersion fluxes in the bulk fluid.

Mass balance:

$$u_f \frac{\partial C_i}{\partial z} = D_r \left(\frac{\partial^2 C_i}{\partial r^2} + \frac{1}{r} \frac{\partial C_i}{\partial r} \right) + D_{e,ax} \frac{\partial^2 C_i}{d z^2} + \rho_f R (C_i, T) \quad (1)$$

Energy balance:

$$u_f \rho_f C_{pf} \frac{d T}{d z} = \lambda_r \left(\frac{\partial^2 T}{\partial r^2} + \frac{1}{r} \frac{\partial T}{\partial r} \right) + \qquad (2)$$

$$\lambda_{e,ax} \frac{d^2 T}{d z^2} + \rho_f (-\Delta H_r) R (C_i, T)$$

Boundary conditions

$$C (r, 0) = C_o \quad ; \quad T (r, 0) = T_o \qquad (3)$$

$$at \quad Z = 0 \quad and \quad 0 \le r \le R$$

$$\frac{\partial C}{\partial r} (0, z) = 0 \quad ; \quad \frac{\partial T}{\partial r} (0, z) = 0 \qquad (4)$$

$$at \quad r = 0 \quad and \quad 0 \le z \le L$$

$$\frac{\partial C}{\partial r} (R, z) = 0 \quad ; \quad \lambda_r \frac{\partial T}{\partial r} (R, z) = U_w (T - T_w) \quad (5)$$

$$at \quad r = R \quad and \quad 0 \le z \le L$$

Conventional two-dimensional heterogeneous model

The models consider the heterogeneity of the reactor i.e the two-phase nature of the reactor. The models account for the difference between the concentration and temperature in the bulk fluid phase and inside the catalyst and the catalyst surface.

Fluid phase for concentration:

$$\frac{\partial C_f}{\partial t} = D_{e,ax} \frac{\partial^2 C_f}{\partial z^2} - U_f \frac{\partial C_f}{\partial z} - \qquad (6)$$

$$\left(\frac{1 - \epsilon_b}{\epsilon_b} \right) \left(\frac{3}{R} \right) k_g (C_f - C_s) \Big|_{r=R}$$

Solid-phase for concentration:

$$\frac{\epsilon_s D_s}{r^2} \frac{\partial}{\partial r} \left(r^2 \frac{\partial C_s}{\partial r} \right) - \rho_s \sum_{i=1}^{n} R_i (C_i, T_i) = \epsilon_s \frac{\partial C_s}{\partial t} \qquad (7)$$

Fluid phase for temperature:

$$\rho_f C_{spf} \frac{\partial T_f}{\partial t} = \lambda_{e,ax} \frac{\partial^2 T_f}{\partial z^2} - U_f \rho_f C_{spf} \frac{\partial T_f}{\partial z} - \tag{8}$$

$$\left(\frac{1-\epsilon_b}{\epsilon_b}\right)\left(\frac{3}{R}\right)\alpha_f\left(T_f - T_s\right)$$

Solid-phase for temperature:

$$\frac{\epsilon_s \lambda_s}{r^2} \frac{\partial}{\partial r}\left(r^2 \frac{\partial T_s}{\partial r}\right) - \rho_s \sum_{i=1}^{n} \Delta H_r R_i\left(C_i, T_i\right) = \tag{9}$$

$$\epsilon_s \rho_s C_{sps} \frac{\partial T_s}{\partial t}$$

Initial and boundary conditions:

(i)　　$C_f = C_o,$　　　$t \leq 0,$　$z_T \geq z \geq 0$ $\tag{10}$

(ii)　　$U_f C_f(t) - U_f C_o\big|_{z=0} + D_{e,ax}\frac{\partial C_f}{\partial z}\bigg|_{z=0} = 0,$　$t > 0$ $\tag{11}$

(iii)　　$\dfrac{\partial C_f}{\partial z}\bigg|_{z=z_T} = 0,$　　$t > 0$ $\tag{12}$

(iv)　　$T_f = T_o,$　　　$t \leq 0,$　$z_T \geq z \geq 0$ $\tag{13}$

(v)　　$U_f \rho_f C_{spf} T_f - U_f \rho_f C_{spf} T_o +$ $\tag{14}$

$$\lambda_{e,ax}\frac{\partial T_f}{\partial z}\bigg|_{z=0} = 0,$$　$t > 0$

(vi)　　$\dfrac{\partial T_f}{\partial z}\bigg|_{z=z_T} = 0,$　　$t > 0$ $\tag{15}$

THEORETICAL SECTION
Mathematical models of catalytic fixed bed tubular reactor

A material balance applied to the bulk fluid phase (macrosystem) gives the following equation:

$$\frac{\partial C_f}{\partial t} = D_{e,ax}\frac{\partial^2 C_f}{\partial z^2} - U_f\frac{\partial C_f}{\partial z} - \tag{16}$$

$$\left(\frac{1-\epsilon_b}{\epsilon_b}\right)\left(\frac{3}{R}\right)k_g\left(C_f - C_s\right)\big|_{r=R}$$

The initial and boundary conditions needed to complete the definition of the macrosystem are:

(i)　　$C_f = C_o,$　　　$t \leq 0,$　$z_T \geq z \geq 0$ $\tag{17}$

(ii) $U_f C_f(t) - U_f C_o\big|_{z=0} + D_{e,ax}\frac{\partial C_f}{\partial z}\bigg|_{z=0} = 0$　$t > 0$ $\tag{18}$

(iii)　　$\dfrac{\partial C_f}{\partial z}\bigg|_{z=z_T} = 0,$　　$t > 0$ $\tag{19}$

The mass transfer effects included in the model are intra-particle diffusion, inter-phase film diffusion, and axial and radial dispersion. The essential assumptions are constant pressure in the reactor because the pressure drop is so small that the initial pressure may be used instead of the reactor pressure at a particular position, constant coefficients of dispersion and diffusion, constant porosities, the constant activity in each catalytic zone, plug flow and the spherical catalyst particles have uniform size and homogeneous structure. Moreover, heat transfer from the fluid phase to the surrounding is included in the energy balance around the column.

The balance for the solid phase is given thus:

$$\frac{\epsilon_s D_s}{r^2}\frac{\partial}{\partial r}\left(r^2 \frac{\partial C_s}{\partial r}\right) - \rho_s \frac{\partial q^*}{\partial t} - \tag{20}$$

$$\rho_s \sum_{i=1}^{n} r'_i\left(C_i, T_i\right) = \epsilon_s \frac{\partial C_s}{\partial t}$$

subject to the following initial and boundary conditions

(i)　　$C_s = 0,$　　　$t = 0,$　$0 \leq r \leq R$ $\tag{21}$

(ii)　　$\dfrac{\partial C_s}{\partial r}\bigg|_{r=0} = 0,$　　　$0 \leq z \leq z_T,$　$t > 0$ $\tag{22}$

(iii)　　$\epsilon_s D_s\left(\dfrac{\partial C_s}{\partial r}\right)\bigg|_{r=R} = k_g\left(C_f - C_s\right),$ $\tag{23}$

$0 \leq z \leq z_T,$　$t > 0$

The energy balance applied to the bulk fluid phase (macrosystem) gives the following equation:

$$\rho_f C_{spf} \frac{\partial T_f}{\partial t} = \lambda_{e,ax}\frac{\partial^2 T_f}{\partial z^2} - U_f\rho_f C_{spf}\frac{\partial T_f}{\partial z} - \tag{24}$$

$$\left(\frac{1-\epsilon_b}{\epsilon_b}\right)\left(\frac{3}{R}\right)\alpha_f\left(T_f - T_s\right) - \frac{a_w}{\epsilon_b}U_w\left(T_f - T_w\right)$$

subject to the initial and boundary conditions:

(i) $T_f = T_o$, $t \leq 0$, $z_T \geq z \geq 0$ (25)

(ii) $U_f \rho_f C_{spf} T_f - U_f \rho_f C_{spf} T_o + \lambda_{e,ax} \left. \dfrac{\partial T_f}{\partial z} \right|_{z=0} = 0$ (26)

$t > 0$

(iii) $\left. \dfrac{\partial T_f}{\partial z} \right|_{z=z_T} = 0$, $t > 0$ (27)

The enthalpy balance for the solid phase is given thus:

$$\frac{\epsilon_s \lambda_s}{r^2} \frac{\partial}{\partial r}\left(r^2 \frac{\partial T_s}{\partial r} \right) - \rho_s \Delta H_{ad} \frac{\partial q^*}{\partial t} - \tag{28}$$

$$\rho_s \sum_{i=1}^{n} \Delta H_r R_i \left(C_i , T_i \right) = \epsilon_s \rho_s C_{sps} \frac{\partial T_s}{\partial t}$$

The initial and boundary conditions needed to complete the definition of Eq. (28) are:

(i) $T_s = T_w$, $t = 0$, $0 \leq r \leq R$ (29)

(ii) $\lambda_s \left(\dfrac{\partial T_s}{\partial r} \right)\Bigg|_{r=R} = \alpha_f \left(T_f - T_s \right)$,   (30)

$0 \leq z \leq z_T$, $t > 0$

(iii) $\left. \dfrac{\partial T_s}{\partial r} \right|_{r=0} = 0$, $0 \leq z \leq z_T$, $t > 0$ (31)

Eq. (28) is the equation that shows the effect of heat generated by adsorption of reactants on the catalyst surface while the second term on the left-hand side of the equation is the representation of the term.

The energy balance around the column wall is given by:

$$\rho_w C_{p,w} \frac{\partial T_w}{\partial t} = - h_w a_w \left(T_w - T_f \right) - \tag{32}$$

$$U_{amb} a_{amb} \left(T_w - T_{amb} \right)$$

Eq. (32) explicitly predicts the effect of the outer-tube wall temperature profile for a given set of inputs, and the effect of heat loss through the wall.

Non-dimensionalization of the model equations

Introducing the dimensionless variables, defined as follows:

$$\overline{C}_i = \frac{C_i}{\left(C_i \right)_o} , \quad \overline{T} = \frac{T}{T_o} , \quad \sigma = \frac{r}{R} ,$$

$$\overline{R}_i \left(\overline{C}_i , \overline{T} \right) = \frac{\left[-r_i'\left(C_i , T \right) \right]}{\left(-r_i' \right)_o \left[\left(C_i \right)_o , T_o \right]} , \overline{Z} = \frac{z}{z_T} , \tau = \frac{t u_f}{z_T}$$

Eq. (16) in dimensionless form gives:

$$\frac{\partial \overline{C}_f}{\partial \tau} = \frac{1}{Pe_m} \frac{\partial^2 \overline{C}_f}{\partial Z^2} - \frac{\partial \overline{C}_f}{\partial Z} - \Phi_1 \left(\overline{C}_f - \overline{C}_s \right)\Big|_{\sigma=1} \tag{33}$$

where

$$Pe_m = \frac{z_T U_f}{D_{e,ax}} \tag{34}$$

$$\Phi_1 = \left(\frac{1-\epsilon_b}{\epsilon_b} \right)\left(\frac{3}{R} \right)\frac{k_g z_T}{U_f} \tag{35}$$

Subject to the transformed initial and boundary conditions:

(i) $\overline{C}_f = 1$ $t \leq 0$, $1 \geq Z \geq 0$ (36)

(ii) $\overline{C}_f (0, \tau) = 1 + \dfrac{1}{Pe_m}\left(\dfrac{\partial \overline{C}_f}{\partial Z} \right)\Bigg|_{Z=0}$ $\tau > 0$ (37)

(iii) $\left. \dfrac{\partial \overline{C}_f}{\partial Z} \right|_{Z=1} = 0$, $t > 0$ (38)

For spherical pellets, Eq. (20) for solid-phase in terms of dimensionless variables yields:

$$\frac{\partial \overline{C}_s}{\partial \tau} = \frac{1}{\Phi_2}\left[\epsilon_s \left(\frac{\partial^2 \overline{C}_s}{\partial \sigma^2} + \frac{2}{\sigma} \frac{\partial \overline{C}_s}{\partial \sigma} \right) - \varphi^2 \overline{R}_i \left(\overline{C}_s , \overline{T}_s \right) \right] \tag{39}$$

where

$$\Phi_2 = \left(1 + \frac{\rho_s q_o^*}{C_o \epsilon_s} \frac{\partial Q^*}{\partial \overline{C}_s} \right) \tag{40}$$

The Thiele modulus, ϕ , is given by

$$\varphi \left\{ = R \sqrt{\frac{\rho_s \left[-r_o'\left(C_o , T_o \right) \right]}{D_s C_o}} \right\} \tag{41}$$

A restatement of the initial and boundary conditions needed to solve Eq. (39) in terms of the dimensionless variables yields:

(i) $\overline{C}_s = 0$, $t \leq 0$, $1 \geq \sigma \geq 0$ (42)

(ii) $\left. \dfrac{\partial \overline{C}_s}{\partial \sigma} \right|_{\sigma = 0} = 0$, $0 \leq Z \leq 1$, $t > 0$ (43)

(iii) $\dfrac{4}{Sh_s} \left(\dfrac{\partial \overline{C}_s}{\partial \sigma} \right)\Big|_{\sigma = 1} = \left(\overline{C}_f - \overline{C}_s \right)\Big|_{\sigma = 1}$,   (44)

$0 \leq Z \leq 1$, $\tau > 0$

Eq. (24) in dimensionless form gives:

$$\dfrac{\partial \overline{T}_f}{\partial \tau} = \dfrac{1}{Pe_h} \dfrac{\partial^2 \overline{T}_f}{\partial Z^2} - \dfrac{\partial \overline{T}_f}{\partial Z} - \Phi_3 \left(\overline{T}_f - \overline{T}_s \right) -$$ (45)

$$\Phi_4 \left(\overline{T}_f - \overline{T}_w \right)$$

where

$$Pe_h = \dfrac{U_f \rho_f C_{spf} z_T}{\lambda_{e,ax}}$$ (46)

$$\Phi_3 = \left(\dfrac{1 - \epsilon_b}{\epsilon_b} \right)\left(\dfrac{3}{R} \right) \dfrac{\alpha_f z_T}{\rho_f C_{spf} U_f}$$ (47)

$$\Phi_4 = \dfrac{a_w U_w z_T}{\epsilon_b \rho_f U_f C_{spf}}$$ (48)

Subject to the transformed initial and boundary conditions:

(i) $\overline{T}_f = 1$, $t \leq 0$, $1 \geq Z \geq 0$ (49)

(ii) $\overline{T}_f(0, \tau) = 1 + \dfrac{1}{Pe_h} \left(\dfrac{\partial \overline{T}_f}{\partial Z} \right)\Big|_{Z=0}$, $\tau > 0$ (50)

(iii) $\left. \dfrac{\partial \overline{T}_f}{\partial Z} \right|_{Z=1} = 0$, $\tau > 0$ (51)

Eq. (28) in dimensionless form yield Eq. (52):

$$\dfrac{\partial \overline{T}_s}{\partial \tau} = \dfrac{1}{\Phi_5} \left[\epsilon_s \left(\dfrac{\partial^2 \overline{T}_s}{\partial \sigma^2} + \dfrac{2}{\sigma} \dfrac{\partial \overline{T}_s}{\partial \sigma} \right) + \beta \varphi^2 \sum_{i=1}^{n} \overline{R}_i \left(\overline{C}_i, \overline{T}_i \right) \right]$$ (52)

where

$$\Phi_5 = \epsilon_s + \dfrac{\Delta H_{ad} q_o^*}{C_{ps} T_o} \dfrac{\partial Q^*}{\partial \overline{T}_s}$$ (53)

$$\beta_s = \dfrac{D_s \left(-\Delta H_{rxn} \right) C_o}{\lambda_s T_o}$$ (54)

The transformed initial and boundary conditions needed to complete the definition of Eq. (52) are:

(i) $\overline{T}_s = 1$, $\tau = 0$, $0 \leq \sigma \leq 1$ (55)

(ii) $\left. \dfrac{\partial \overline{T}_s}{\partial \sigma} \right|_{\sigma = 0} = 0$, $0 \leq Z \leq 1$, $\tau > 0$ (56)

(iii) $\dfrac{4}{Nu} \left(\dfrac{\partial \overline{T}_s}{\partial \sigma} \right)\Big|_{\sigma = 1} = \left(\overline{T}_f - \overline{T}_s \right)$,   (57)

$0 \leq Z \leq 1$, $\tau > 0$

The linear adsorption isotherm used in computation has the form:

$$q^* = a_L C$$ (58)

In dimensionless form, we have equations:

$$\dfrac{\partial Q^*}{\partial \overline{C}_s} = \dfrac{a_L C_o}{q_o^*},$$ (59)

Which are used in equations (40) to obtain simple expressions Φ_2.

For an ideal gas, $pV = nRT \Rightarrow p = CRT$, that is $C = p/RT$. Using this relationship in Eq.(59) and introducing dimensionless variables, we obtain:

$$\dfrac{\partial Q^*}{\partial \overline{C}_s} = \dfrac{a_L C_o}{q_o^*},$$ (60)

Which are used in Eq. (53) to obtain an expression for Φ_5.

The dimensionless energy balance equation around the column wall is given by:

$$\dfrac{\partial \overline{T}_w}{\partial \tau} = -\dfrac{h_w a_w z_T}{\rho_w C_{p,w} U_f} \left(\overline{T}_w - \overline{T}_f \right) -$$ (61)

$$\dfrac{U_{amb} a_{amb} z_T}{\rho_w C_{p,w} U_f} \left(\overline{T}_w - \overline{T}_{amb} \right)$$

### Application of the model to partial oxidation of methanol to formaldehyde

In this study, the exothermic reaction chosen was from the pilot plant experimental work of *Windes et al.* [19], which involves the partial oxidation of methanol to formaldehyde accompanied by a side reaction of formaldehyde

Table 1: The geometric, kinetic and parameters used for the partial oxidation of methanol to formaldehyde.

Physical properties and bed characteristics	value	unit
Fluid density	1000	[kg/m3]
Catalyst density	2000	[kg/m3]
Wall density	7800	[kg/m3]
Specific heat of the fluid	952	[J/kg-K]
Specific heat of the catalyst	1904	[J/kg-K]
Thermal conductivity of the fluid	2.0	[W/m-K]
Superficial velocity	2.47	[m/s]
Feed temperature	523	[K]
Methanol in feed	1.7	[mol/m3]
Oxygen in feed	34	[mol/m3]
Fluid Temperature	523	[K]
Wall temperature	523	[K]
Ambient temperature	523	[K]
Reactor tube radius	0.0133	[m]
Particle diameter	0.0046	[m]
Thermal conductivity of the catalyst	2.0	[W/(m.K)]
Thermal conductivity of the bulk fluid	0.08	[W/(m.K)]
Void fraction in the bed	0.5	
Void fraction in particles	0.57	
Length of the reactor	0.7	[m]
Particle effective diffusivity	4.9×10^{-6}	[m2/s]
Effective axial diffusivity	0.2619	[m2/s]
Ratio of mean surface area to volume of the column		
Wall	270.0	[m-1]
Ratio of internal surface area to volume of the column		
Wall	300.0	[m-1]
Heat transfer coefficient from wall to ambient	7.092	[W/(m2.K)]
Heat transfer coefficient from the fluid to solid phase	400	[W/(m2.K)]
Heat transfer coefficient of the wall	528	[W/(m2.K)]
Overall heat transfer coefficient of the wall	220	[W/(m2.K)]
Inlet pressure	1.55	[atm.]
Outlet pressure	1.3	[atm.]
Kinetic parameters		
Heat of reaction for reaction 1	-158700	[J/mole]
Heat of reaction for reaction 2	-158700	[J/mole]
Heat of adsorption	- 8368	[J/mole]
Dimensionless number		
Peclet number (mass)	6.6	
Peclet number (heat)	8.6	
Sherwood number	11.0	
Biot number	5.5	

to carbon monoxide and water. This is a consecutive side reaction over an iron oxide/molybdenum oxide catalyst.

The chemical reaction is as follows:

$$CH_3OH + \frac{1}{2}O_2 \rightarrow HCHO + H_2O \qquad (62)$$
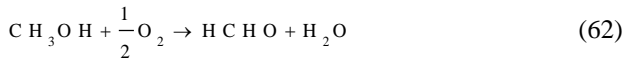
with the rate expression:

$$(-r_M) = \frac{k_1 C_M^{0.5}}{1 + K_2 C_M^{0.5}}; \quad k_1 = 125 \times 10^7 \exp\left(-\frac{79496}{RT}\right); \quad (63)$$

$$K_2 = 1.12 \exp\left(-\frac{8368}{RT}\right)$$

This is accomplished with an undesirable side reaction.

$$CH_2O + \frac{1}{2}O_2 \rightarrow CO + H_2O \qquad (64)$$

$$(-rCH_2O) = \frac{k_2 C_{CH_2O}^{0.5}}{1 + 0.2 C_{CH_2O}^{0.5}}; \quad k_2 = \qquad (65)$$

$$54 \times 10^5 \exp\left(-\frac{8368}{RT}\right)$$

These values of constants and parameters were taken from the experimental work of *Windes et al.* [19] and to which the simulation results were compared.

Rendering the rate Eq. (63) for the partial oxidation of methanol to formaldehyde in dimensionless forms, and using the resulting expressions in Eq. (39), we have:

$$\frac{\partial \overline{C}_s}{\partial \tau} = \qquad (66)$$

$$\frac{1}{\Phi_2}\left[\epsilon_s\left(\frac{\partial^2 \overline{C}_s}{\partial \sigma^2} + \frac{2}{\sigma}\frac{\partial \overline{C}_s}{\partial \sigma}\right) + \varphi_s^2 \frac{\exp\left[\frac{\beta_1 \gamma_1(1-\overline{C}_s)}{1+\beta_1(1-\overline{C}_s)}\right]\overline{C}_s^{0.5}}{DEN1}\right]$$

Introducing dimensionless reaction term to Eq. (52),

$$\frac{\partial \overline{T}_s}{\partial \tau} = \qquad (67)$$

$$\frac{1}{\Phi_5}\left[\epsilon_s\left(\frac{\partial^2 \overline{T}_s}{\partial \sigma^2} + \frac{2}{\sigma}\frac{\partial \overline{T}_s}{\partial \sigma}\right) + \beta_1 \varphi_s^2 \frac{\exp\left[\frac{\beta_1 \gamma_1(1-\overline{C}_s)}{1+\beta_1(1-\overline{C}_s)}\right]\overline{C}_s^{0.5}}{DEN1}\right]$$

Where

$$\beta_1 = \frac{(-\Delta H_{rxn})D_s C_o}{\lambda_s T_o}; \quad \gamma_1 = \frac{E_1}{R_g T_o}; \quad \gamma_2 = \frac{\Delta H_2}{R_g T_o}$$

$$\varphi_s = R\sqrt{\frac{\rho_b k_{1o}}{D_s C_o^{0.5}}\exp(-\gamma_1)}$$

$$DEN1 = \left[1 + k_{2o}\exp(-\gamma_2)C_o^{0.5}\exp\left[\frac{\gamma_2 \beta_2(1-\overline{C}_s)}{1+\beta_2(1-\overline{C}_s)}\right]|\overline{C}_s^{0.5}\right]$$

Methods for the numerical solution

The numerical method adopted for the solution of the mass and enthalpy balance equations is the method of orthogonal or optimal collocation. The orthogonal collocation method is applied by first choosing a new set of dimensionless variables, which have values lying between 0 and 1.

When the method of orthogonal collocation is applied to the space variables Z and σ then substituting $u = \sigma^2$, Eq. (33) becomes:

$$\frac{d\overline{C}_{fj}}{d\tau} = \sum_{k=2}^{N+1}\overline{W}_{j,k}\overline{C}_{fk} - \sum_{k=1}^{NR}A'_{N+1,k}\overline{C}_{pk} - \qquad (68)$$

$$\Phi_1(1-\Phi_6)\overline{C}_{fj} + \overline{P}e_m$$

Where

$$\overline{W}_{j,k} = \frac{1}{Pe_m}\left(B_{j,1}A'_{1,k} + B_{j,N+2}A''_{1,k} + B_{j,k}\right) - \qquad (69)$$

$$\left(A_{j,1}A'_{1,k} + A_{j,N+2}A''_{1,k} + A_{j,k}\right)$$

$$\overline{P}e_m = \frac{1}{Pe_m}\left(Pe'_m B_{j,1} + Pe''_m B_{j,N+2}\right) - \qquad (70)$$

$$\left(Pe'_m A_{j,1} + Pe''_m A_{j,N+2}\right)$$

$$Pe'_m = \frac{\dfrac{Pe_m}{A_{1,N+2}}}{\dfrac{Pe_m}{A_{1,N+2}} - \dfrac{A_{1,1}}{A_{1,N+2}} + \dfrac{A_{N+2,1}}{A_{N+2,N+2}}}$$

$$A'_{1,k} = \frac{\dfrac{A_{1,k}}{A_{1,N+2}} - \dfrac{A_{N+2,k}}{A_{N+2,N+2}}}{\dfrac{Pe_m}{A_{1,N+2}} - \dfrac{A_{1,1}}{A_{1,N+2}} + \dfrac{A_{N+2,1}}{A_{N+2,N+2}}}$$

$$Pe_m'' = \frac{\dfrac{Pe_m}{A_{1,1} - Pe_m}}{\dfrac{A_{N+2,N+2}}{A_{N+2,1}} - \dfrac{A_{1,N+2}}{A_{1,1} - Pe_m}} \quad ; \quad A_{1,k}'' = \frac{\dfrac{A_{1,k}}{A_{1,1} - Pe_m} - \dfrac{A_{N+2,k}}{A_{N+2,1}}}{\dfrac{A_{N+2,N+2}}{A_{N+2,1}} - \dfrac{A_{1,N+2}}{A_{1,1} - Pe_m}}$$

$$\Phi_6 = \frac{1}{1 + \dfrac{4}{Sh_i} A_{N+1,N+1}} \quad ; \quad A_{N+1,k}' = \frac{4}{Sh_s} A_{N+1,k} \Phi_9$$

Also, by applying orthogonal collocation to the system model equations for the spherical particle radial direction, we have

$$\frac{\partial \overline{C}_{sj}}{\partial \tau} = \tag{71}$$

$$\frac{1}{\Phi_2} \left[\in_s \left(\sum_{k-1}^{NR} F_{j,k} \overline{C}_{sk} + \Phi_6 \Phi_7 \overline{C}_{fj} \right) + \varphi_s^2 \frac{\exp\left[\dfrac{\beta_1 \gamma_1 \left(1 - \overline{C}_{sj}\right)}{1 + \beta_1 \left(1 - \overline{C}_{sj}\right)} \right] \overline{C}_{sj}^{0.5}}{DEN1} \right]$$

Where

$$\overline{F}_{j,k} = \left[4u_j \left(B_{j,k} - B_{j,N+1} A_{N+1,k}' \right) + \tag{72} \right.$$

$$\left. 6 \left(A_{j,k} - A_{j,N+1} A_{N+1,k}' \right) \right]$$

$$\Phi_7 = \left(4u_j B_{j,N+1} + 6A_{j,N+1} \right) \tag{73}$$

Following the same development of the collocation points for the concentration profiles in the bulk fluid phase and solid phase, the resulting expressions for the temperature profiles in these phases are presented thus:

$$\frac{d\overline{T}_{fj}}{d\tau} = \sum_{k=2}^{N+1} \overline{H}_{j,k} \overline{T}_{fk} - \sum_{k=1}^{NR} A_{N+1,k}^* \overline{T}_{sk} - \tag{74}$$

$$\left(\Phi_3 - \Phi_3 \Phi_8 + \Phi_4 \right) \overline{T}_{fj} + \overline{Pe}_h + \Phi_4 \overline{T}_w$$

$$\frac{\partial \overline{T}_s}{\partial \tau} = \frac{1}{\Phi_3} \left[\in_s \left(\sum_{k=1}^{NR} \overline{U}_{j,k} \overline{T}_{sk} + \Phi_7 \Phi_8 \overline{T}_{fj} \right) + \tag{75} \right.$$

$$\beta_1 \varphi_s^2 \frac{\exp\left[\dfrac{\beta_1 \gamma_1 \left(1 - \overline{C}_s\right)}{1 + \beta_1 \left(1 - \overline{C}_s\right)} \right] \overline{C}_{sj}^{0.5}}{DEN1} \left. \right]$$

Where

$$\overline{H}_{j,k} = \frac{1}{Pe_h} \left(B_{j,1} A_{1,k}''' + B_{j,N+2} \tilde{A}_{1,k} + B_{j,k} \right) - \tag{76}$$

$$\left(A_{j,1} A_{1,k}''' + A_{j,N+2} \tilde{A}_{1,k} + A_{j,k} \right)$$

$$\overline{U}_{j,k} = \left[4u_j \left(B_{j,k} - B_{j,N+1} A_{N+1}^* \right) + \tag{77} \right.$$

$$6 \left(A_{j,k} - A_{j,N+1} A_{N+1}^* \right)$$

$$\overline{Pe}_h = \frac{1}{Pe_h} \left(Pe_h' B_{j,1} + Pe_h'' B_{j,N+2} \right) - \tag{78}$$

$$\left(Pe_h' A_{j,1} + Pe_h'' A_{j,N+2} \right)$$

$$\Phi_7 = \left(4u_j B_{j,N+1} + 6A_{j,N+1} \right) \tag{79}$$

$$Pe_h' = \frac{\dfrac{Pe_h}{A_{1,N+2}}}{\dfrac{Pe_h}{A_{1,N+2}} - \dfrac{A_{1,1}}{A_{1,N+2}} + \dfrac{A_{N+2,1}}{A_{N+2,N+2}}}$$

$$A_{1,k}''' = \frac{\dfrac{A_{1,k}}{A_{1,N+1}} - \dfrac{A_{N+2,k}}{A_{N+2,N+2}}}{\dfrac{Pe_h}{A_{1,N+2}} - \dfrac{A_{1,1}}{A_{1,N+2}} + \dfrac{A_{N+2,1}}{A_{N+2,N+2}}}$$

$$Pe_h'' = \frac{\dfrac{Pe_h}{A_{1,1} - Pe_h}}{\dfrac{A_{N+2,N+2}}{A_{N+2,1}} - \dfrac{A_{1,N+2}}{A_{1,1} - Pe_h}}$$

$$\tilde{A}_{1,k} = \frac{\dfrac{A_{1,k}}{A_{1,1} - Pe_h} - \dfrac{A_{N+2,k}}{A_{N+2,1}}}{\dfrac{A_{N+2,N+2}}{A_{N+2,1}} - \dfrac{A_{1,N+2}}{A_{1,1} - Pe_h}}$$

$$\Phi_8 = \frac{1}{1 + \dfrac{4}{Nu_s} A_{N+1,N+1}} \quad ; \quad A_{N+1,k}^* = \frac{4}{Nu_s} A_{N+1,k} \Phi_8$$

RESULTS AND DISCUSSION

The results of the reaction network investigated is presented and discussed in this section.

The effects of heat generated by adsorption of the reactants on the catalyst and heat loss by the wall on the magnitude of hotspot temperature using partial oxidation of methanol to formaldehyde on FeO/MoO_3 catalyst were discussed.

Temperature and concentration profiles in the reactor

Figs. 1 and 2 show the temperature and concentration profiles for the experimental work, the simulated model, the conventional heterogeneous model without the effect of heat generated by adsorption of reactants on the catalyst surface, and the pseudo-homogeneous model in the axial direction of the reactor for the partial oxidation of methanol to formaldehyde and water. In Fig. 1, excellent agreement was achieved between the experimental data for the partial oxidation of methanol to formaldehyde on FeO/MoO_3 catalyst and simulated results. The proposed model predicted the location of the hotspot at the same dimensionless distance of 0.4413 (= 0.0309 m) as the experimental value but with a temperature of 619 K as compared with the experimental value of 622 K having an Absolute Average Deviation (AAD) ±0.48%. The conversion of methanol for the models shows a faster conversion of the methanol to formaldehyde even before reaching the half of the reactor as a result of high temperature. The conventional heterogeneous model predicted the magnitude of the hotspot temperature to be about 8 K lower than the experimental value at the same location with the experimental result. This thus shows that heat generated by adsorption of the reactants on the catalyst surface has a major effect on the magnitude of the hotspot. A temperature difference of such magnitude will lead to a runaway effect which can lead to deleterious effects in the reactor like undesired side reactions, catalyst deactivation by sintering and productivity loss, and reduction of product selectivity. The pseudo-homogeneous model predicted the magnitude of the hotspot temperature to be 34K lower than the experimental value. The model shows a gradual conversion of methanol with a prolonged reaction which is normally the point of runaway condition but was been predicted as a steady temperature variation. Fig. 2 shows the concentration profiles of the methanol conversion for the experimental work, the simulated model, and the conventional heterogeneous model without the effect of the heat of adsorption isotherm and the pseudo-homogeneous model in the axial direction of the reactor. Just like in the temperature profiles, the experimental work, simulated model, and conventional heterogeneous model showed that complete conversion takes place at a dimensionless distance of 0.4413 at the location of the hotspot. This shows that at the hotspot temperature, the methanol concentration is almost zero, and at this point
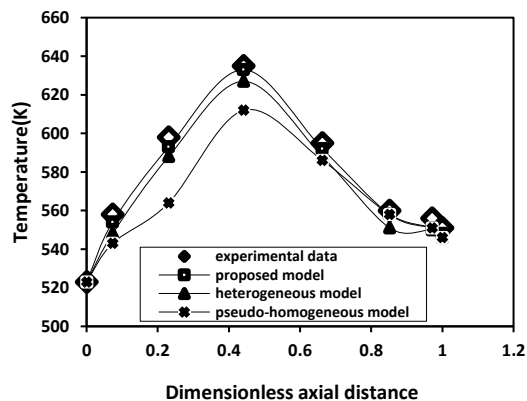

Fig. 1: The axial temperature profiles of different models developed in the reactor.
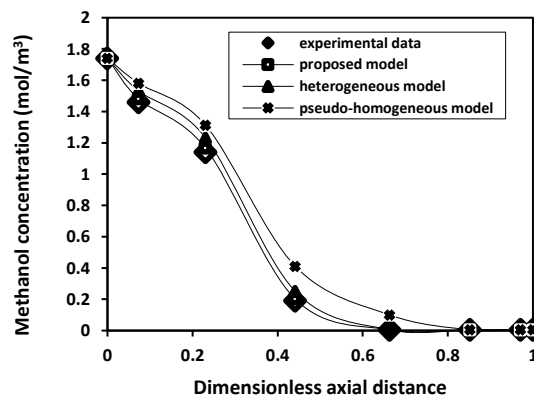

Fig. 2: The axial concentration profiles of different models developed in the reactor.

the undesired product is being produced as the reaction is a consecutive one. The formaldehyde produced is converted to carbon monoxide and water. The pseudo-homogeneous model predicted a stretched concentration profile up to a dimensionless concentration of about 0.8 very close to the exit of the reactor [14].

Effect of change in wall temperature and wall heat transfer coefficient on hotspot

Fig. 3 shows the effect of change in the wall temperature on the magnitude of hotspot temperature as predicted from the developed model Eq. (61). As the wall temperature decreases from 523 K to 493 K the hotspot temperature drops from 622 K to 589.12 K. This shows that 1 K decrease in wall temperature leads to 1.1 K drop in hotspot temperature. Fig. 4 depicts the effect of change in the heat transfer coefficient of the wall on the

hotspot temperature at the prevailing condition. A ten times increase in the magnitude of h_w from 528.0 W/m²K to 5280.0 W/m²K leads to about 8 K drop in hotspot temperature showing that h_w has a major effect on the amount of heat transfer through the wall. As the value of h_w increases the reaction being exothermic loses heat to the surroundings through the bed wall thus reducing the temperature in the reactor column.

Response of the reactor to change in feed temperature, wall temperature, and feed concentration.

Fig. 5 shows the response of the reactor to change in the feed temperature from 503 K to 523 K. There is an increase in the hotspot temperature from about 593 K to 622 K with the location of the hotspot moving closer to the entrance of the reactor. This means an increase in feed temperature leads to an increase in the reaction rate leading to methanol being consumed very close to the entrance of the reactor compared to feed temperature of 503 K which has its location of the hotspot at a dimensionless axial distance of 0.667 which is closer to the exit [20]. Figs. 6 and 7 show the response of the reactor to changes in the wall temperature and feed concentration (methanol) from 503 K to 523 K and 1.74 mol/m³ to 1.914 mol/m³ respectively. There is an increase in the temperature throughout the reactor with the greatest effect at the location of the hotspot with little or no change in the position of the hotspot for the two changes.

Variation of the temperature inside the catalyst pellet and with time along the reactor

Fig. 8 depicts the variation of the temperature inside the catalyst pellet. The reaction being exothermic leads to decrease in temperature from the center of the pellet to the outer surface of the catalyst as heat is released to the surroundings. Although the increase in the feed temperature leads to an increase in the temperature inside the catalyst pellet [14]. Fig. 9 shows the transient change in the reactor. There is an initial increase in the temperature inside the reactor after which the temperature becomes steady as time goes on [14, 21].

CONCLUSIONS

A detailed and feasible mathematical model for a porous heterogeneous catalytic fixed bed tubular reactor has been developed. The model consists of hyperbolic
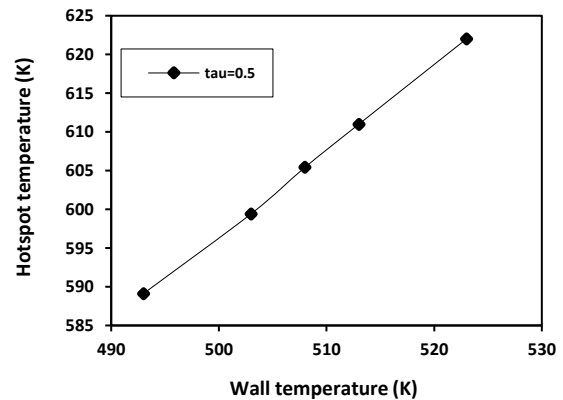

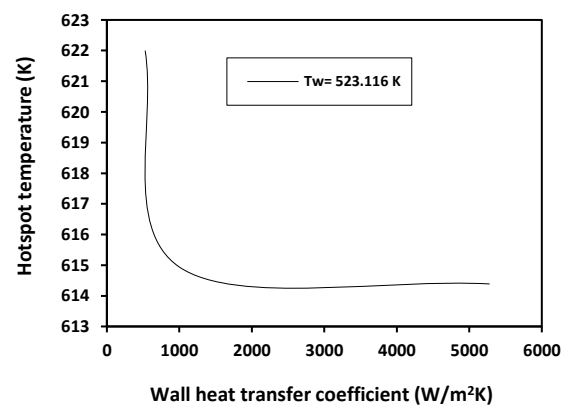**Fig. 3: Effect of change in wall temperature on hotspot temperature (time is 3mins)**

Fig. 4: Effect of change in wall heat transfer coefficient on hotspot temperature.
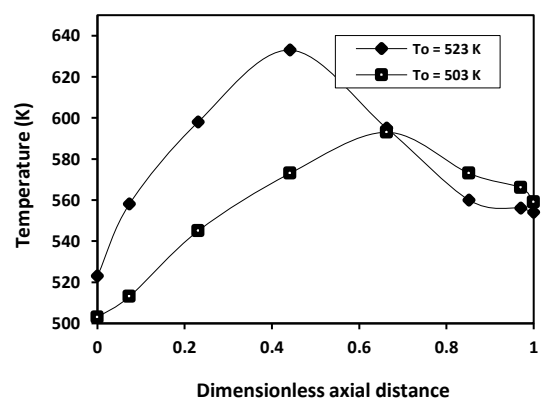

Fig. 5: Response of the reactor to change in feed temperature from 503 K to 523 K.
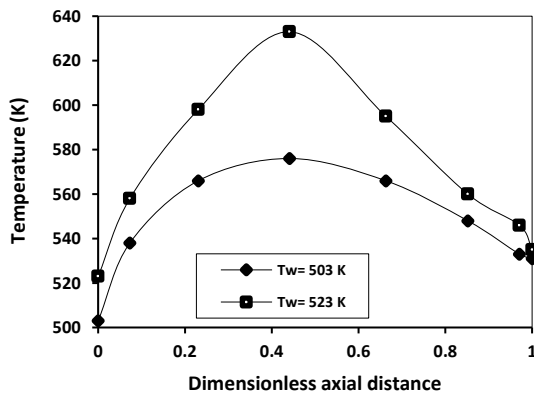
Fig. 6: Response of the reactor temperature to change in wall temperature from 503 K to 523 K.
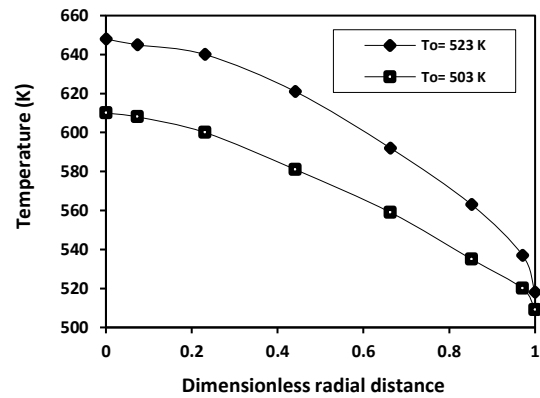

Fig. 8: Temperature profiles inside the catalyst pellet at different feed temperatures (503K and 523K).
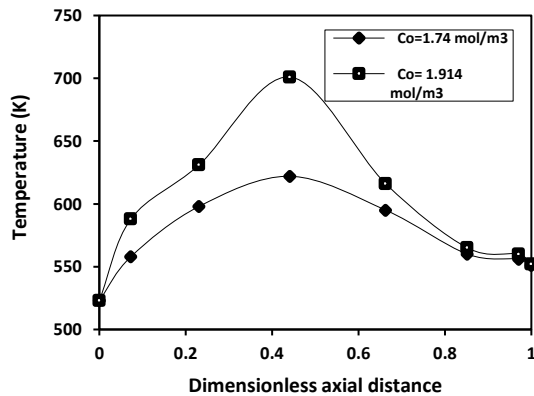

Fig. 7: Response of the reactor temperature to change in feed concentration (methanol).
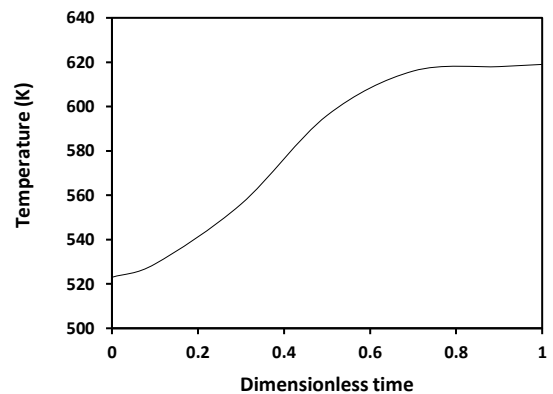

Fig. 9: Temperature variation with time in the reactor.

and parabolic partial differential equations took into account intra-particle and inter-particle diffusion resistances; heat generated by adsorption of reactants on the catalyst surface and the heat transfer from the fluid phase to the surroundings was included in the energy balance as it has a significant effect on the reactor performance, especially reactor "hotspot". The model shows that heat generated by adsorption of reactants on the catalyst surface has an effect on the magnitude of the hotspot and reducing the temperature of the column wall leads to a decrease in the magnitude of the hotspot. An increase in the value of the wall heat transfer coefficient leads to an appreciable reduction in the magnitude of the hotspot. It also shows that the model was able to accurately predict the experimental result of the reaction system, suggesting that the developed model represents the essential features of the real system. The comprehensive

model developed herein is useful in the design and analysis of a catalytic packed bed tubular reactor, where mass and heat transfer resistances are accounted for.

Acknowledgments

Nomenclature

a_{amb}	Ratio of mean surface area to volume of the column wall, m^{-1}
a_F	Freundlich adsorption isotherm constant, m^3/kg
a_L	Langmuir adsorption isotherm constant, m^3/kg
a_w	Ratio of internal surface area to volume of the column wall, m^{-1}

$A_{j,k}$	Constant generated in the orthogonal collocation method
AAD	Absolute average deviation
b_L	Langmuir adsorption isotherm constant, m^3/kg
$B_{j,k}$	Constant generated in the orthogonal collocation method
C_f	Concentration of solute in fluid phase of the column, mol/m^3
$\bar{C}_f$	Dimensionless concentration of solute in the bulk fluid phase of the reactor, C_f/C_o
C_s	Concentration in the solid phase, mol/m^3
C_{sp}	Specific heat capacity, $J/(kg\ K)$
C_o	Inlet concentration of solute in the bulk fluid phase of the reactor, mol/m^3
$D_{e,ax}$	Effective axial diffusivity of solute in the fluid phase, m^2/s
D_s	Effective diffusivity of solute in catalyst pellet, m^2/s
E_A	Activation energy, J/mol
ΔH	Heat of reaction, J/mol
ΔH_{ad}	Heat of adsorption, J/mol
k_g	Mass transfer coefficient from the fluid to pore-fluid phase, m/s
k_o	Frequency (or pre-exponential) factor, s^{-1}
h_{fs}	Heat transfer coefficient from the fluid to pore-fluid phase, $W/(m^2\ K)$
h_w	Heat transfer coefficient from the fluid to the wall, $W/(m^2\ K)$
K_p	Adsorption rate coefficient, s^{-1}
n	Freundlich adsorption isotherm exponent
N	Number of interior collocation points in the axial direction
NR	Number of collocation points in the radial direction
Nu	Nusselt number, $2\alpha_f R / \lambda_p$
Pe_h	Peclet number (heat), $U_f z_T \rho_f C_{spf} / \lambda_f$
Pe_m	Peclet number (mass), $U_f z_T / D_{e,ax}$, dimensionless
q^*	Concentration of solute in the solid (or adsorbed) phase, mol/m^3
q_o^*	adsorbed solute concentration at equilibrium with fluid phase concentration, C_o, mol/m^3
Q^*	Dimensionless concentration of solute in the solid (or adsorbed) phase, q^*/q_o^*
R	External radius of the pellet, m
R_g	Universal gas constant, $kJ/(kmol\ K)$
$R_i(C_i,T_i)$	Reaction rate of solute, $kg/(m^3\ s)$
r	Radial distance in the pellet, m
Sh_s	Sherwood number of solute in catalyst pellet, dimensionless
T_a	Ambient temperature, K
T_f	Temperature of solute in the fluid phase, K
T_s	Tmperature of solute in the catalyst pellet, K
T_o	Inlet temperature of solute in the reactor, K
$\bar{T}_f$	Dimensionless temperature
T_s^*	Catalyst surface temperature in equilibrium with pore-fluid phase, K
T_w	Temperature at reactor wall, K
t	Time, s
U_{anb}	Heat transfer coefficient from wall to ambient, $W/(m^2\ K)$
U_f	Interstitial velocity, m/s
U_w	Overall heat transfer coefficient of the wall, $W/(m^2\ K)$
V_i	Stoichiometric coefficient of component i in reaction i, dimensionless
z	Axial distance in the column, m
z_T	Total length of reactor, m
Z	Dimensionless length of reactor, z/z_T

Greek Letters

α_f	Heat transfer coefficient from the fluid to the solid phase, $W/(m^2\ K)$
$\in_b$	The void fraction in the bed (i.e. volume of voids per unit volume of bed), dimensionless
$\in_s$	The void fraction in particles (i.e. volume of pores in the pellet per unit volume of pellet), dimensionless
λ	Effective thermal conductivity
η	Effectiveness factor, dimensionless
ρ	Density, kg/m^3
σ	Dimensionless radius, r/R
$\tau_{(tau)}$	Dimensionless time, tU_f/z_T
$\phi\ \varphi$	Thiele modulus

Superscript

*	Equilibrium value

Subscript

f	Fluid phase

i, j, k	Integer values
s	Solid phase
w	Wall

REFERENCES

[1] Kursawe A., "Partial Oxidation of Ethene in Microchannel Reactor. Catalytic Pellet Reactor", Ph.D. Thesis, Technische Universiat Chemnizt, Fakulat fur Naturwissenschat, (2009).

[2] LL'in H., Luss D., Wrong-Way Behaviour of Packed Bed Reactors: Influence of Reactant Adsorption on Support, *AIChE. Journal*, **38**: 1609-1617 (1992).

[3] Bolis V.," Fundamentals in Adsorption at the Solid-Gas Interface, Concepts and Thermodynamics". CA. Aurox (Ed.) Springer-Verlag Berlin Heidelberg, (2013).

[4] Ahmed A., Fahien R.W., Tubular Reactor Design I, Two Dimensional Model, *Chemical Engineering Science*, **35**: 889-895 (1978).

[5] Linke D., Wolf D., Baerns M., Zeyb S., Dingerdissen U., Mleczko, L., Catalytic Partial Oxidation of Ethane to Acetic Acid over $Mo_1V_{0.25}Nb_{0.12}Pd_{0.0005}Ox$; Reactor Operation, *Chemical Engineering Science*,**57**: 39-51 (2002).

[6] Aboudheir A., Akande A., Idem R., Dalai A., Experimental Studies and Comprehensive Reactor Modelling of Hydrogen by Catalytic Reforming of Crude Ethanol in a Packed Bed Tubular Reactor over a Ni/Al_2O_3 Catalysts, *International Journal of Hydrogen Energy*, **31**: 752-761 (2006).

[7] Amin N.S, Istadi., Yee, N.P., Mathematical Modelling of Catalytic Fixed-Bed Reactor for Carbon Dioxide Reforming of Methane over Rh/Al_2O_3 Catalyst. Bulletin of Chemical Reaction Engineering Catalysis,**3(1-3)**: 21-29 (2008).

[8] Jess A., Kern, C., Modelling of Multi-Tubular Reactor for Fischer Tropsch Synthesis, *Chemical Engineering Technology*, **35**: 1164-1175 (2009).

[9] Suh J., Lee M., Greif R., Grogoropoulos C.P., Transport Phenomena in a Steam-Methanol Reforming Microreactor with Internal Heating, *International Journal of Hydrogen Energy,***34**: 314 – 322 (2009).

[10] Lassak P., Labovsky J., Jelemensky L., Influence of Parameter Uncertainty in Modelling of Industrial ammonia Reactor for Safety and Operability Analysis, *Journal of Loss Prevention in the Process Industries,***35**: 280-288 (2010).

[11] Vasco de Toledo E.C., Morais E.R., Melo D.N.C., Mariano A.P., Meyer Jao F.C. A., Maciel Filho R., Suiting Dynamic Models of Fixed-Bed Catalytic Reactors for Computer Based Applications, *Engineering*, **3**: 778-785 (2011).

[12] Mahinsa P., Sadeghi M.T., Ganji H., Shokri S., Modeling and Sensitivity Analyses of Hydrodesulfurization Catalyst Pellet, *Petroleum and Coal,***54(2)**: 104 –109(2012).

[13] Sadooghi P., Rauch R., Pseudo-homogeneous Modeling of Catalytic Methane Reforming Process in a Fixed Bed Reactor, *Journal of Natural Gas Science and Engineering,***11**: 46-51 (2013).

[14] Fischer K.L., Langer M.R., Freund H., Dynamic Carbon Dioxide Methanation in a Wall-Cooled Fixed Bed reactor: Comparative Evaluation of Reactor Models, *Ind. Res. Chem. Res.,* **58(42)**: 19406-19420 (2019).

[15] Liu Q.S., Zhang Z.L., Zhou J.L., Steady State and Dynamic Behaviour of Fixed Bed Catalytic Reactor for Fischer-Tropsch Synthesis I: Mathematical Model and Numerical Method, *Journal of Natural Gas Chemistry,* **8(2)**: 137-180 (1999).

[16] Celia X., "Catalytic Pellet Reactor Design under Uncertainty", Laboratory for Product and Process Design (LPPD). Project Final Report, University of Illinois at Chicago, (2005).

[17] Cornelio A.A., Dynamic Modeling of an Industrial Ethylene Oxide Reactor, *Indian Chemical Engineering. Section A,* **48(3)**: 117-135 (2006).

[18] Vasco de Toledo E.C., Morais E.R., Stremel D.P., Meyer F.C. A., Maciel Filho R., *Development of Rigorous and Reduced Heterogeneous Dynamic Models for Fixed Bed Catalytic Reactor and Three-Phase Catalytic Slurry Reactor, Chemical Products and Process Modelling,***3**: 1-45 (2008).

[19] Windes L. C., Schwedock M. J., Ray W.H., Steady State and Dynamic Modeling of a Packed Bed Reactor for the Partial Oxidation of Methanol to Formaldehyde I. Model Development, *Chemical Engineering Communication*, **78:**1-43 (1989).

Research Article

[20] Zhu J., Araya S. S., Cui X., Sahlin S.L., Kaer S.K., Modeling and Design of a Multi-Tubular Packed-Bed Reactor for Methanol Steam Reforming over a $Cu/ZnO/Al_2O_3$ Catalyst, *Energies*, **13:** 610-635 (2020).

[21] Bendjaouahdou C., Bendjaouahdou M. H., Control of the Hotspot Temperature in an Industrial SO_2 Converter, *Energy Procedia*, **36:** 428-443 (2013).